CrystEngComm

Accepted Manuscript

This article can be cited before page numbers have been issued, to do this please use: P. F. M. Filho Marques de Oliveira, A. A.L. Michalchuk, J. Marquardt, T. Feiler, C. Prinz, R. M. Torresi, P. Camargo and F. Emmerling, *CrystEngComm*, 2020, DOI: 10.1039/D0CE00826E.

ROYAL SOCIETY OF CHEMISTRY

rsc.li/crystengcomm

View Article Online
DOI: 10.1039/D0CE00826E

ARTICLE

Investigating the Role of Reducing Agents on Mechanosynthesis of Au Nanoparticles

Received 00th January 20xx,
Accepted 00th January 20xx

DOI: 10.1039/x0xx00000x

Paulo F M de Oliveira,*[a,b] Adam A L Michalchuk,[b] Julien Marquardt,[b] Torvid Feiler,[b] Carsten Prinz,[b] Roberto M Torresi,[a] Pedro H C Camargo,[a,c] and Franziska Emmerling*[b]

Control over the bottom up synthesis of metal nanoparticles (NP) depends on many experimental factors, including the choice of stabilising and reducing agents. By selectively manipulating these species, it is possible to control NP characteristics through solution-phase synthesis strategies. It is not known, however, whether NPs produced from mechanochemical syntheses are governed by the same rules. Using the Au NPs mechanosynthesis as a model system, we investigate how a series of common reducing agents affect both the reduction kinetics and size of Au NPs. It is shown that the relative effects of reducing agents on mechanochemical NPs synthesis differ significantly from their role in analogous solution-phase reactions. Hence, strategies developed for control over NPs growth in solution are not directly transferrable to environmentally benign mechanochemical approaches. This work demonstrates a clear need for dedicated, systematic studies on NPs mechanosynthesis.

Introduction

Metal nanoparticles (NPs) with controlled size and shape can be synthesised efficiently through bottom-up (BU) approaches[1–4]. These synthesis strategies involve the chemical reduction of a metal precursor, typically in solution, followed by nucleation and growth of the NPs. Correspondingly, a reducing agent must be selected to drive the transformation. Moreover, BU methods typically require a stabilising agent to inhibit aggregation of NPs and overgrowth. Whereas the reducing agent affects the rate of chemical reduction, the stabilising agent can selectively promote the preferential exposure of specific surface facets in the produced NPs. In solution, careful selection of these two additives has allowed for control over NPs morphologies.[5] Highly anisotropic nanostructures have been successfully obtained, including rods, plates, rattles, and urchins.[6–14] This shape control has allowed tuning of NP properties for applications in catalysis,[9,12,13,15] optics and sensing,[7,16–18] and biomedicine.[14,19]

Mechanochemical approaches are well-known for their applications in metallurgical,[20] mineralogical,[21] and chemical sciences.[22] Recently, BU noble metal NP syntheses have been also demonstrated using mechanochemical means, e.g. for Au, Ag, and Pd NPs.[23–28] In the reported examples, common reducing agents such as sodium borohydride ($NaBH_4$) and sodium citrate (Ctr) were used, along with polyvinylpyrrolidone (PVP) as a stabilizing agent. Examples are also known where PVP[24,25] and a support material such as lignin[27] or eggshell[29,30] can act as the reducing agent. NP bottom up mechanosyntheses (BUMS) have also been demonstrated in which the metallic milling assembly facilitates reduction of the metal oxidized species through galvanic replacement.[26] With increased routes available for NP BUMS, elucidating the effect of reducing agent is of growing importance.

The mechanisms and rates of mechanochemical transformations are known to depend on many experimental parameters, including the milling device, mechanical energy input, milling balls, and milling ball/jar materials.[31–33] Under select configurations, analytical and numerical models for the kinetics of inorganic mechanochemical transformations have been reported.[31,32,34] These models have included general consideration of mixing,[35,36] stress relaxation,[37] and comminution rates.[38] The rate-limiting importance of each of these factors is system-dependent.[39–42] Moreover, in some cases the apparent rate may be instead limited by the chemical transformation itself. Understanding which factors limit the apparent rates in specific reaction types – for example BUMS – is crucial to gain control over their transformations.

To date, only a limited number of studies have attempted to extract meaningful kinetic constants for the preparation of nanoscale materials. One example is the synthesis of TlCl nanoparticles, where the mass-transfer coefficient was estimated for a solid system in an AGO-2 mill.[43,44] To the best of our knowledge, only a single study has so far attempted to address the kinetics of BUMS, even at a purely qualitative level. In our recent work, we explored the BUMS of Au NPs using

[a] Departamento de Química Fundamental, Instituto de Química, Universidade de São Paulo. Av. Lineu Prestes 748, 05508000, São Paulo, Brazil. E-mail: paulofmo@usp.br.
[b] BAM Federal Institute for Materials Research and Testing, Richard-Willstätter-Strasse 11, 12489 Berlin, Germany. E-mail: franziska.emmerling@bam.de
[c] Department of Chemistry, University of Helsinki, A.I. Virtasen aukio 1, Helsinki, Finland.
† Footnotes relating to the title and/or authors should appear here.
Electronic Supplementary Information (ESI) available: Experimental details and methods. See DOI: 10.1039/x0xx00000x

tandem *in situ* time-resolved X-ray absorption spectroscopy and diffraction.[45]

Au NPs are technologically relevant materials with several applications, including in catalysis and medicine.[19,46] Au NPs have been traditionally prepared using high temperature, solvent-intensive approaches.[47–49] There is growing interest in their mechanochemical syntheses. Control of NP synthesis *via* mechanochemical routes requires the identification of suitable conditions for seed generation and subsequent NP growth. Both seed formation and growth depend critically on the reducing agent selected for BUMS. The effect of reducing agents on these processes are well known in solution.[5] However, the lessons learned from solution-phase syntheses do not translate to mechanochemical conditions. Studies dedicated to gaining control over NP BUMS are therefore required.

Using Au NP synthesis as a model system, the present study aims to better elucidate how reducing agents affect the BUMS of NPs. Specifically, we unravel how the role of the reducing agent in BUMS differs from their influence on established solution-phase approaches. These results can thus illustrate the possibility to exploit existing knowledge from solution chemistry to expedite the development of mechanochemical approaches for shape-controlled NPs.

Experimental Methods

Materials. All materials were obtained from commercial suppliers: AuCl (99.9 %, Sigma-Aldrich), hydroquinone (99 %, Acros Organics), sodium citrate dihydrate (99 %, Sigma-Aldrich), L-ascorbic acid (99%, Sigma-Aldrich), $NaBH_4$ (98 %, Fischer Chemical) and polyvinylpyrrolidone (PVP; $\overline{Mw}$ 10,000 g.mol^{-1}, Sigma-Aldrich). In each case, the material was used as-supplied, without further purification.

Mechanosynthesis. The mechanochemical synthesis of AuNPs was performed in a vibratory ball mill (P23, Fritsch), operating at 50 Hz using a single zirconia ball (ø = 10 mm, 3.0 g) and a 10 mL PMMA jar. AuNPs were prepared by chemical reduction of AuCl in the presence of a reducing agent (R_A) and PVP as the stabilising agent. The relative amounts of AuCl and R_A are given in Table 1 for each synthesis strategy. Compositions were derived from the corresponding balanced redox equations (Eq. S8-S11, S2-S15, ESI), in which the stoichiometry is determined by the balance of electron transfer. For each synthesis, the total mass of the powder mixture (150 mg) was kept constant, ensuring the ball-to-mass ratio was not a contributing factor to relative rates of NP synthesis. Moreover, the same amount of PVP (100 mg) was added to each run, minimising its role in determining NP synthesis rates. The R_As were premilled with PVP to improve their dispersion in the media and reduce particle size effects before the addition of AuCl.

Analytical Methods. All mechanochemically prepared powders were analysed by *ex situ* powder X-ray diffraction (PXRD) immediately following mechanochemical treatment (see ESI S2.2). This ensured negligible aging of the sample between synthesis and analysis. PXRD were collected using a Bruker D8 Advance (Bruker AXS GmbH, Germany) in Bragg-Brentano geometry using Cu Kα ($\lambda = 1.5406$ Å) and a Ni filter. Diffraction data were collected over a range of 15-80° 2θ (step width 0.02° 2θ, count time 1 s/step, total collection time 55 min). This elongated collection time has negligible effect on sample aging (see ESI SX).Where data quality was sufficient, quantitative Rietveld refinement was performed using FullProf Suite 3.0.0 (details in ESI, S2.3).[50] HighScorePlus suite[51] (3.0e) was used to treat the powder diffraction data and to extract the integrated peak intensities.

Electron Transmission Microscopy (TEM) images were obtained using a Talos F200S microscope (Thermo Scientific) operating at 200 kV. The solid samples were dispersed in isopropanol, deposited in Carbon-Formvar coated Cu grids and dried in air.

Table 1. Composition of mixtures used for mechanochemical synthesis of AuNPs. The Ideal Molar Ratio (IMR) based on the reduction of 1 mol of Au^+, Experimental Molar Ratio (EMR), Mass Ratio (M_WR), Mass Fraction (M_WF) are given.

R_A	IMR[a]	EMR[b]	M_WR	AuCl M_WF[c]	R_A M_WF[c]
$NaBH_4$	1:1/8	1:1/4	24.25	0.324	0.013
AA	1:1/2	1.1	1.32	0.190	0.144
HQ	1:1/2	1:1	2.11	0.227	0.107
Ctr	1:1/6	1:1/3	2.34	0.235	0.100
		1:1/2	1.56	0.203	0.130
		1:1	0.79	0.147	0.187
		1:2	0.39	0.094	0.240

[a]Stoichiometric ratio, according to equations Eq S12-S15 (ESI), to reduce one mol of Au^I. [b]Molar ratio used in the experiments – in all cases the reducing agents were used in excess. [c]Overall mass fraction including PVP (100 mg) + AuCl + R_A.

Results and Discussion

The chemical reduction of AuCl under ball milling conditions was performed in the presence of PVP. Reducing agents (R_A) commonly used in solution were selected for the reaction and include $NaBH_4$, ascorbic acid (AA), hydroquinone (HQ) and sodium citrate dihydrate (Ctr), Fig. 1.

The general chemical equation for the BUMS reactions explored in this work follows

$$\mathrm{AuCl} + \mathrm{R}_A \rightarrow \mathrm{AuNP} + \mathrm{R}_{A(ox)} + \mathrm{XCl} \qquad \text{Eq. 1}$$

where X=H or Na from the R_A. According to the standard electrochemical cell potentials (ΔE^0_{cell}, Eq. S6) and Gibbs Free

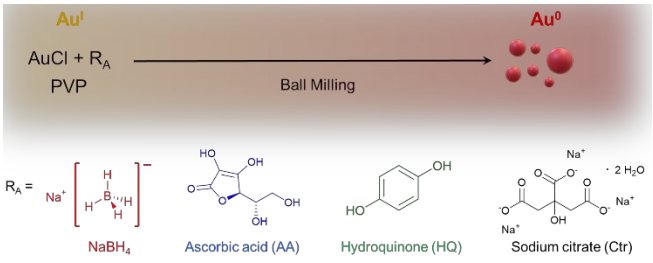

Fig. 1. AuNPs formation in ball milling conditions from the chemical reduction of AuCl (Au^I salt) using different reducing agents (R_A) – sodium borohydride (NaBH4), ascorbic acid (AA), hydroquinone (HQ) and sodium citrate dihydrate (Ctr) – and polyvinylpyrrolidone (PVP) as stabilizing agent.

Energy (ΔG, Eq. S7), the chemical reaction is thermodynamically favoured for all reducing agents (R_A) used here (Table 1) (Table S2, ESI).

In solution, it is expected that the rate of Au^I reduction (Eq. 1) decreases with the cell potential and hence the choice of R_A .[5,52–54] This follows from the general acceptance that, according to Marcus Theory, solution-phase electron-transfer reaction rates are guided by the redox pair potential.[5,52–54] Therefore, the solution-phase reaction rates should follow according to R_A as $NaBH_4$ (ΔE^0_{cell}= + 2.311 V) > AA (ΔE^0_{cell}= + 1.753 V) > HQ (ΔE^0_{cell} = + 1.131 V) > Ctr (ΔE^0_{cell}= + 0.599 V). Correspondingly, this trend is used as a benchmark against which to explore the apparent rate of reaction under ball milling conditions.

During Au NP mechanosynthesis, a multi-modal distribution of crystallite sizes was obtained. This led to significant distortion of the powder X-ray diffraction (PXRD) peak shapes. Correspondingly, reliable quantitative Rietveld refinements needed special considerations and were made difficult for these reactions. Moreover, we opted not to add an internal standard thereby avoiding inadvertent seeding of NP growth. The negligible scattering of PVP and the reducing agents allowed us to instead develop a calibration curve for quantitative assessment based on the Rietveld refinement of reactions using R_A=$NaBH_4$. The Au^0 and AuCl mass fractions obtained by Rietveld refinement were correlated against the ratio of the integrated peak intensities ($I_{(hkl)}$) of Au^0 and AuCl (See ESI S2.4).

The apparent rates of NP formation during the mechanosynthesis for all four reducing agents ($NaBH_4$, HQ, AA, and Ctr) are given in Fig. 2. Each synthesis exhibits an induction period, an acceleration or growth phase, and a deceleration. These trends are consistent with our previously reported time-resolved *in situ* monitoring of a similar Au NPs mechanosynthesis.[45] Moreover, these dominant kinetic features are consistent with other mechanochemical transformations – e.g. cocrystal and salt formation,[55–58] and covalent bond-forming reactions[59–62] – suggesting the same physical effects guide the apparent macroscopic rate of Au NP BUMS. The magnitude of the induction period depends markedly on the choice of R_A, following as HQ < AA < $NaBH_4$ < Ctr, Fig. 2. Correspondingly, the rate of Au NP mechanosynthesis follows the reverse order.

From the trends displayed in Fig. 2 it becomes immediately apparent that the relative rates of Au NP BUMS do not mimic those that are known for solution-phase transformations. Most notably, HQ which is a relatively mild R_A in solution reaction, becomes the fastest BUMS reaction, such that the apparent BUMS rates follow as R_A=HQ > AA >> $NaBH_4$ > Ctr. $NaBH_4$ is known in solution to be amongst the strongest reducing agents. Under BUMS conditions, $NaBH_4$ instead exhibits only mild reducing power. Moreover, unlike reactions with R_A=AA, HQ and Ctr, the reaction performed with R_A=$NaBH_4$ remains incomplete even after 8 h of ball milling. Ctr is a mild R_A at room temperature in aqueous solution and generally requires heat for efficient reduction. In contrast Ctr does not require explicit heat under BUMS conditions to reduce Au^I, although it is still a considerable weaker R_A. It is evident that the conditions of BUMS do not reflect those of solution phase NP synthesis. We suggest the unique BUMS trends to stem – at least in part – from the varied interaction between the R_A and the PVP polymer matrix. AA and PVP are known to form a stable solid dispersion, thereby readily distributing AA throughout the powder mixture.[63] Similarly, HQ also interacts favourably with the organic matrix moieties.[64,65] As such, intimate mixing of both AA and HQ throughout the powder is presumably facile. In contrast, the ionic character of R_A Ctr and $NaBH_4$ are not expected to interact strongly with organic PVP. Correspondingly, these R_A are presumably poorly mixed in the reaction mixture, limiting contact formation. Correlations between the affinity of R_A with the polymer matrix and the associated macroscopic kinetics deserve dedicated investigations.

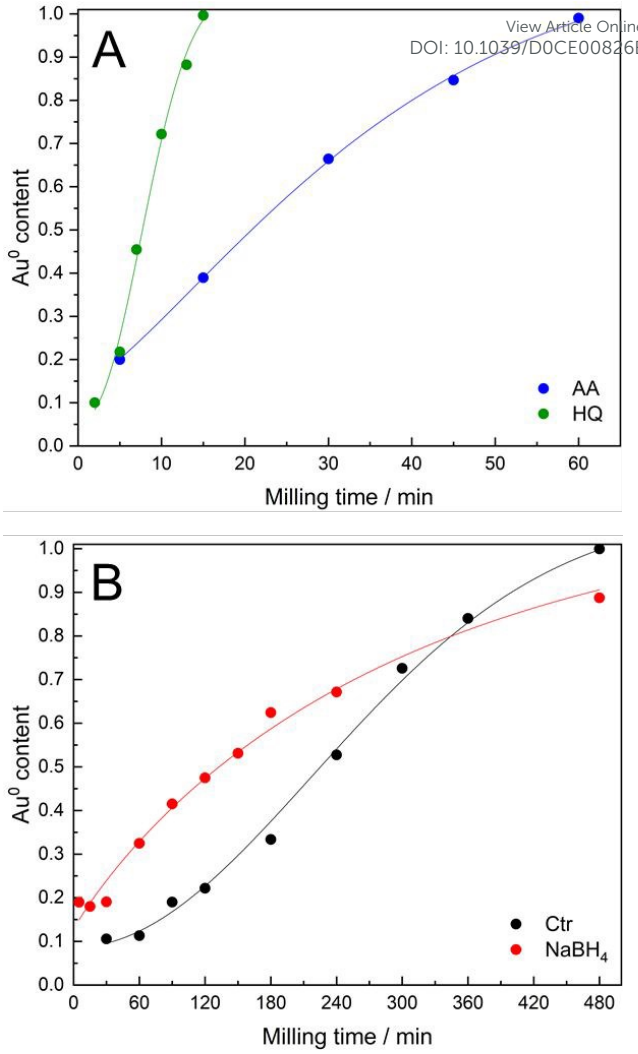

Fig. 2. Apparent rates of AuCl reduction towards Au NP formation. Reactions are shown for (A) RA=AA and HQ; (B) RA=Ctr (AuCl:Ctr molar ratio 1:1/3), NaBH4. The initial reaction compositions are shown in Table 1. Each data point corresponds to an independent run measured directly afterwards. The lines correspond to the fit to Eq. S17.

Solution phase kinetics are dominated by ready thermally induced diffusion of reacting species. The mixing and collision terms associated with such reactions are often minimal and

encompassed in a semi-empirical 'pre-exponential' term of the Arrhenius equation. In ball milling transformations, however, the treatment becomes less obvious. It is generally accepted that mechanical action can adopt a variety of roles. For multi-phase reactions, this role is typically to facilitate intimate mixing *via* comminution and mass transport. The apparent kinetic profile of BUMS is especially complex and at the macroscopic level follows the general scheme,

$$A + B \xrightarrow{k_1} A \cdots B \xrightarrow{k_2} C \xrightarrow{k_3} D \qquad \text{Eq. 2}$$

That is to say that physical contacts between the metal precursor and reducing agent must first be formed (A+B). This process itself is a convolution of macroscopic mixing and comminution. The chemical redox process subsequently occurs (A…B), followed by agglomeration/aggregation of reduced metal atoms (C) to form NPs (D). Owing to the inherent instability of individual reduced metal atoms, this general transformation scheme can be only monitored by detection of D or low of A+B. Correspondingly, the apparent rate of reaction is proportional to some combination of at least three macro-elementary steps. Deconvoluting the role physical mixing (k_1), the chemical reaction (k_2) and NP growth (k_3) remains an open question. Understanding this problem in further detail is crucial for garnering control of NP bottom up mechanosynthesis, including for size and shape control.

Owing to the complexity of unravelling the elementary stages of ball milling reactions, it is convenient to instead discuss a macroscopic (or apparent) rate constant, *k'*, where

$$k' \propto f(k_1, k_2, k_3, \ldots) \qquad \text{Eq. 3}$$

Such that the overall macroscopic transformation (α) can be described according to a general equation,

$$\alpha = 1 - e^{(-k' t^n)} \qquad \text{Eq. 4}$$

A fit of the experimental data (Fig. 2) to Eq. 4 (in the form of Eq S17, ESI) offers a route to extract apparent macroscopic rate constants for the BUMS reactions. We note that given the limited dataset, no meaningful mechanistic information can be readily obtained from a fit to this generic equation (see ESI S2.5 for discussion). However, the quality fit does confirm that Au BUMS follows conventional solid-state macroscopic kinetics.

As a proof of concept, and attempting to unravel the complexity of Eq. 4, we explored further the BUMS with R_A=Ctr as a model system. Like all R_A, Ctr is the limiting reagent in Eq. 1. Correspondingly, we posit that increasing the mass fraction of Ctr should reduce the rate limiting nature of mixing (*i.e.* of k_1 in Eq. 2). To this end, the amount of Ctr used in the Au NP BUMS was varied systematically. Additional to the electrochemically balanced ratio AuCl:Ctr 1:1/3 (twice the ideal Ctr content, Table 1), we tested also AuCl:Ctr ratios of 1:1/2; 1:1 and 1:2 (Fig. 3). Based on the based on the per Au atom reduction equations (ESI, Eq. S12-S15), these represent 1.5-, 3- and 6-fold increases relative Ctr to Au ratio, respectively.

By increasing the relative amount of Ctr, so it was the BUMS reaction rate successfully increased, Fig. 3. A fit of each dataset to Eq. 4 (fitting *only* the rate constant *k,* see ESI S2.5*)* suggests

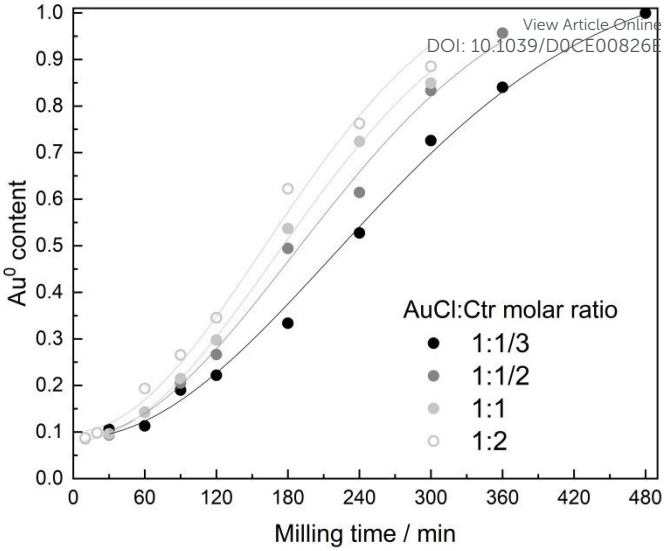

Fig. 3. Trends of AuCl reduction towards Au NPs formation using different AuCl:Ctr molar ratios: 1:1/3; 1:1/2; 1:1; and 1:2. Each point corresponds to an independent run measured immediately afterwards. The lines correspond to the fit to Eq. S17.

that the macroscopic rate constants follow as: $k'_{1:1/3} = 1.05 \times 10^{-5}$, $k'_{1:1/2} = 1.46 \times 10^{-5}$ $k'_{1:1} = 1.76 \times 10^{-5}$ and $k'_{1:2} = 1.97 \times 10^{-5}$ min^{-2}, for AuCl:Ctr 1:1/3, 1:1/2, 1:1 and 1:2, respectively. Although these data correspond to increases in the relative mass of Ctr by 50%, 100%, and again 100%, the accompanying increase in reaction rate follows as 40%, 20%, and 11%. It is therefore clear that the effect of increasing the quantity of the limiting reagent Ctr is asymptotic in rate, thereby eliminating the contribution of mixing to BUMS macroscopic kinetics.

Comparing macroscopic mechanochemical kinetics requires isolating individual reaction components where possible. However, although we demonstrate the suppression of mixing on the rate BUMS, direct comparison of the resulting curves remains complicated. Under these conditions, the relative concentrations of reagents are no longer conserved, and additional corrections for corresponding effects must be made. This further highlights the considerable complexity associated with investigating macroscopic 'kinetics' of ball milling transformations.

The Au NPs obtained under each BUMS reaction conditions were analysed by TEM (Fig.4). Quasi-spherical nanosized Au particles with broad size distribution were obtained regardless of the R_A used in the synthesis. $NaBH_4$ (Fig.4A) and AA (Fig.4B) produced NPs of similar size and distribution: 10.8 ± 5.0 nm and 11.9 ± 4.0 nm, respectively. Using HQ as R_A (Fig.4C) yielded the largest and most irregular NPs for any of the tested R_A, having a mean size of 17.1 ± 8.9 nm. In contrast, Ctr with a AuCl:Ctr molar ratio of 1:1/3 generated the smallest Au NPs (Fig 4D) with an overall mean size of 6.6 ± 4.8 nm. The particle size distribution for Ctr is more appropriately represented by two families of NPs with sizes of *ca.* 3 nm and 12 nm (Fig.S8-D, ESI).

In the colloidal synthesis of metal NPs, the choice of metal salt-R_A pair can influence the size, shape, and even the composition of product NPs the case of multimetallic

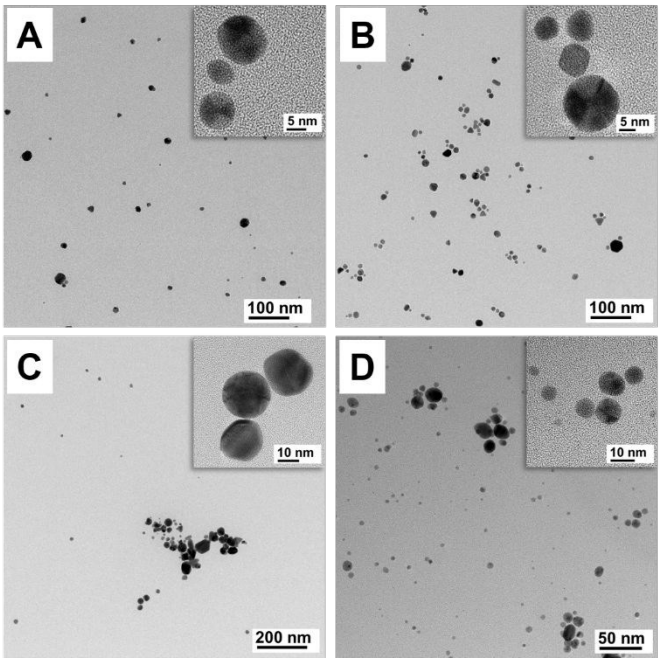

Fig. 4. TEM images of the AuNPs synthesized in milling conditions using the NaBH4 (A), AA (B), HQ (C) and Ctr (D) as reducing agents. Size distribution histograms can be found in ESI (Fig.S8).

systems.[5,66] Strong R_A –a prototypical example, $NaBH_4$ – typically yield small NPs (often < 5 nm) as a result of rapid reduction kinetics.[5] The uncontrolled growth of these small NPs offers poor control over NP geometry, but provides a useful route for the preparation of NP seeds. Controlled NP growth from such seeds typically requires a mild reducing agent, such as Ctr, AA and HQ in solution. Slower reduction conditions allow for controlled atom addition thereby yielding a variety of shapes in proper conditions.

These rules for R_A dependent NP control have been established in solution. However, it is evident from the present work that these rules do not hold for BUMS. HQ led to fast reduction kinetics (Fig.2), yet produced large NPs (Fig4A). In contrast, Ctr exhibited very slow BUMS kinetics (Fig.2), but produced the smallest NPs (Fig.4D). The small NPs obtained with Ctr unlikely result from particle comminution. It is known that prolonged milling times drive NP aggregation and fusion, thereby increasing particle sizes.[23,28] Nonetheless it is worth mentioning that Ctr may also participate in the stabilizationNPs.[67]

Conclusions

The bottom-up mechanosynthesis of Au NPs from AuCl was studied in the presence of four different reducing agents: $NaBH_4$, ascorbic acid (AA), hydroquinone (HQ), and sodium citrate (Ctr). In solution, the relative strength (and hence rate of reduction) of these reducing agents typically follows as $NaBH_4$ > AA > HQ > Ctr. Importantly, this trend is not reproduced when considering the relative effect of reducing agent on Au NP mechanosynthesis, instead following as HQ > AA > Ctr > $NaBH_4$.

$NaBH_4$ is the strongest (hence fastest) reducing agent in solution. In contrast, under BUMS conditions, $NaBH_4$ is the slowest reducing agent and is the only agent which does not lead to complete reduction of the AuCl starting material. In contrast, HQ exhibits only a mild (*i.e.* slower) reduction strength in solution but led to complete reduction of AuCl with only 15 minutes under BUMS conditions. Similarly, insights from solution phase NP synthesis suggest that faster reduction leads to smaller NPs. In contrast, we demonstrate in this work that the speed of AuCl reduction under BUMS conditions does not directly correlate to the size of the resulting NPs. The slowest reducing agent under BUMS conditions – $NaBH_4$ – also yields the smallest NPs. In contrast, the largest NPs are produced under BUMS conditions with the fastest reducing agent: HQ. It follows that the general rules developed for controlling NP synthesis in solution do not hold for their mechanosynthesis.

Ball milling transformations of solids are extraordinarily complex. factors which influence the rates and mechanisms of these solid-phase reactions are counterintuitive when considered under the paradigm of solution chemistry. It is evident here that the mechanosynthesis of NPs are no exception. Dedicated studies must be carried out to better elucidate the factors which control NP synthesis under BUMS conditions. Only in this way can the true potential of these environmentally benign strategies be fully realised for preparation of technologically relevant controlled NP materials.

Acknowledgements

PFMO thanks the Sao Paulo Research Foundation (FAPESP) (FAPESP 2017/15456-0 and 2019/01619-0) and RMT for Grant (FAPESP 2015/26308-7).

Conflicts of interest

There are no conflicts to declare.

Notes and references

1 Y. Xia, Y. Xiong, B. Lim and S. E. Skrabalak, *Angew. Chemie Int. Ed.*, 2009, **48**, 60–103.
2 P. H. C. Camargo, T. S. Rodrigues, A. G. M. da Silva and J. Wang, in *Metallic Nanostructures*, eds. Y. Xiong and X. Lu, Springer International Publishing, Cham, 2015, pp. 49–74.
3 K. D. Gilroy, A. Ruditskiy, H.-C. Peng, D. Qin and Y. Xia, *Chem. Rev.*, 2016, **116**, 10414–10472.
4 A. R. Tao, S. Habas and P. Yang, *Small*, 2008, **4**, 310–325.
5 T. S. Rodrigues, M. Zhao, T. Yang, K. D. Gilroy, A. G. M. da Silva, P. H. C. Camargo and Y. Xia, *Chem. – A Eur. J.*, 2018, **24**, 16944–16963.
6 S. E. Lohse and C. J. Murphy, *Chem. Mater.*, 2013, **25**, 1250–1261.
7 J. Reguera, J. Langer, D. Jiménez de Aberasturi and L. M. Liz-Marzán, *Chem. Soc. Rev.*, 2017, **46**, 3866–3885.
8 Y. Pei, L. Huang, J. Wang, L. Han, S. Li, S. Zhang and H. Zhang, *Nanotechnology*, 2019, **30**, 222001.

9 H. Liu, P. Zhong, K. Liu, L. Han, H. Zheng, Y. Yin and C. Gao, *Chem. Sci.*, 2018, **9**, 398–404.
10 Z. Fan, X. Huang, C. Tan and H. Zhang, *Chem. Sci.*, 2015, **6**, 95–111.
11 Y. Sun, B. Wiley, Z.-Y. Li and Y. Xia, *J. Am. Chem. Soc.*, 2004, **126**, 9399–9406.
12 J. Quiroz, E. C. M. Barbosa, T. P. Araujo, J. L. Fiorio, Y.-C. Wang, Y.-C. Zou, T. Mou, T. V. Alves, D. C. de Oliveira, B. Wang, S. J. Haigh, L. M. Rossi and P. H. C. Camargo, *Nano Lett.*, 2018, **18**, 7289–7297.
13 A. G. M. da Silva, T. S. Rodrigues, V. G. Correia, T. V. Alves, R. S. Alves, R. A. Ando, F. R. Ornellas, J. Wang, L. H. Andrade and P. H. C. Camargo, *Angew. Chemie Int. Ed.*, 2016, **55**, 7111–7115.
14 D. Maysinger, A. Moquin, J. Choi, M. Kodiha and U. Stochaj, *Nanoscale*, 2018, **10**, 1716–1726.
15 T. S. Rodrigues, A. G. M. da Silva and P. H. C. Camargo, *J. Mater. Chem. A*, 2019, **7**, 5857–5874.
16 J. Langer, S. M. Novikov and L. M. Liz-Marzán, *Nanotechnology*, 2015, **26**, 322001.
17 C. J. Murphy, T. K. Sau, A. M. Gole, C. J. Orendorff, J. Gao, L. Gou, S. E. Hunyadi and T. Li, *J. Phys. Chem. B*, 2005, **109**, 13857–13870.
18 E. Hao, G. C. Schatz and J. T. Hupp, *J. Fluoresc.*, 2004, **14**, 331–341.
19 X. Yang, M. Yang, B. Pang, M. Vara and Y. Xia, *Chem. Rev.*, 2015, **115**, 10410–10488.
20 C. Suryanarayana, *Prog. Mater. Sci.*, 2001, **46**, 1–184.
21 P. Baláž, *Int. J. Miner. Process.*, 2003, **72**, 341–354.
22 S. L. James, C. J. Adams, C. Bolm, D. Braga, P. Collier, T. Friščić, F. Grepioni, K. D. M. Harris, G. Hyett, W. Jones, A. Krebs, J. Mack, L. Maini, a G. Orpen, I. P. Parkin, W. C. Shearouse, J. W. Steed and D. C. Waddell, *Chem. Soc. Rev.*, 2012, **41**, 413–47.
23 D. Debnath, S. H. Kim and K. E. Geckeler, *J. Mater. Chem.*, 2009, **19**, 8810.
24 D. Debnath, C. Kim, S. H. Kim and K. E. Geckeler, *Macromol. Rapid Commun.*, 2010, **31**, 549–553.
25 T. Premkumar and K. E. Geckeler, *Colloids Surfaces A Physicochem. Eng. Asp.*, 2014, **456**, 49–54.
26 M. J. Rak, A. Moores, N. K. Saadé, T. Friščić and A. Moores, *Green Chem.*, 2013, **16**, 86–89.
27 M. J. Rak, T. Friščić and A. Moores, *Faraday Discuss.*, 2014, **170**, 155–167.
28 P. F. M. de Oliveira, J. Quiroz, D. C. de Oliveira and P. H. C. Camargo, *Chem. Commun.*, 2019, **55**, 14267–14270.
29 B. J. Tiimob, G. Mwinyelle, W. Abdela, T. Samuel, S. Jeelani and V. K. Rangari, *J. Agric. Food Chem.*, 2017, **65**, 1967–1976.
30 M. Baláž, N. Daneu, Ľ. Balážová, E. Dutková, Ľ. Tkáčiková, J. Briančin, M. Vargová, M. Balážová, A. Zorkovská and P. Baláž, *Adv. Powder Technol.*, 2017, **28**, 3307–3312.
31 F. K. Urakaev and V. V. Boldyrev, *Powder Technol.*, 2000, **107**, 197–206.
32 F. K. Urakaev and V. V. Boldyrev, *Powder Technol.*, 2000, **107**, 93–107.
33 F. K. h. Urakaev, in *High-Energy Ball Milling - Mechanochemical processing of nanopowders*, ed. M. Sopicka-Lizer, Woodhead Publishing, 2010, pp. 9–44.
34 E. Avvakumov, M. Senna and N. Kosova, *Soft Mechanochemical Synthesis: A Basis for New Chemical Technologies*, Kluwer Academic Publishers, Boston, 2002.
35 O. V. Lapshin, V. V. Boldyrev and E. V. Boldyreva, *Russ. J. Phys. Chem. A*, 2019, **93**, 1592–1597.
36 O. V. Lapshin, V. K. Smolyakov, E. V. Boldyreva and V. V. Boldyrev, *Russ. J. Phys. Chem. A*, 2018, **92**, 66–69.
37 A. P. Chupakhin, A. A. Sidel'nikov and V. V. Boldyrev, *React. Solids*, 1987, **3**, 1–19.
38 F. Delogu and G. Cocco, *J. Mater. Synth. Process.*, 2000, **8**, 271–277.
39 P. Y. Butyagin, *Colloid J. Russ. Acad. Sci. Kolloidn. Zhurnal*, 2003, **65**, 648–651.
40 P. Y. Butyagin, *Phys. Solid State*, 2005, **47**, 856.
41 P. Y. Butyagin, *Russ. Chem. Rev.*, 1971, **40**, 901–915.
42 S. N. Zhurkov, *Int. J. Fract.*, 1984, **26**, 295–307.
43 F. K. Urakaev, *Mendeleev Commun.*, 2012, **22**, 215–217.
44 F. K. Urakaev, *Mendeleev Commun.*, 2012, **22**, 103–105.
45 P. F. M. de Oliveira, A. Michalchuk, A. de O. G. Buzanich, R. Bienert, R. M. Torresi, P. H. C. . Camargo and F. Emmerling, *ChemRxiv*, , DOI:10.26434/chemrxiv.12290756.v1.
46 M. Stratakis and H. Garcia, *Chem. Rev.*, 2012, **112**, 4469–4506.
47 J. Turkevich, P. C. Stevenson and J. Hillier, *Discuss. Faraday Soc.*, 1951, **11**, 55.
48 G. Frens, *Nat. Phys. Sci.*, 1973, **241**, 20–22.
49 F. Fievet, J. P. Lagier and M. Figlarz, *MRS Bull.*, 1989, **14**, 29–34.
50 J. Rodriguez-Carvajal, *Full Prof suite 3.0.0, Lab. Leon Brillouin, CEA-CNRS, 2003*.
51 T. Degen, M. Sadki, E. Bron, U. König and G. Nénert, *Powder Diffr.*, 2014, **29**, S13–S18.
52 R. A. Marcus, *Angew. Chemie Int. Ed. English*, 1993, **32**, 1111–1121.
53 T. P. Silverstein, *J. Chem. Educ.*, 2012, **89**, 1159–1167.
54 J. D. S. Newman and G. J. Blanchard, *Langmuir*, 2006, **22**, 5882–5887.
55 M. R. Caira, L. R. Nassimbeni and A. F. Wildervanck, *J. Chem. Soc. Perkin Trans. 2*, 1995, 2213.
56 A. A. L. Michalchuk, K. S. Hope, S. R. Kennedy, M. V. Blanco, E. V. Boldyreva and C. R. Pulham, *Chem. Commun.*, 2018, **54**, 4033–4036.
57 A. A. L. Michalchuk, I. A. Tumanov, S. Konar, S. A. J. Kimber, C. R. Pulham and E. V. Boldyreva, *Adv. Sci.*, 2017, **4**, 1700132.
58 I. Halasz, A. Puškarič, S. a J. Kimber, P. J. Beldon, A. M. Belenguer, F. Adams, V. Honkimäki, R. E. Dinnebier, B. Patel, W. Jones, V. Štrukil and T. Friščič, *Angew. Chemie - Int. Ed.*, 2013, **52**, 11538–11541.
59 H. Kulla, S. Haferkamp, I. Akhmetova, M. Röllig, C. Maierhofer, K. Rademann and F. Emmerling, *Angew. Chemie - Int. Ed.*, 2018, **57**, 5930–5933.
60 A. M. Belenguer, A. A. L. Michalchuk, G. I. Lampronti and J. K. M. Sanders, *Beilstein J. Org. Chem.*, 2019, **15**, 1226–1235.

View Article Online
DOI: 10.1039/D0CE00826E

61 S. Haferkamp, A. Paul, A. A. L. Michalchuk and F. Emmerling, *Beilstein J. Org. Chem.*, 2019, **15**, 1141–1148.
62 P. F. M. Oliveira, N. Haruta, A. Chamayou, B. Guidetti, M. Baltas, K. Tanaka, T. Sato and M. Baron, *Tetrahedron*, 2017, **73**, 2305–2310.
63 J. O. Sanchez, Y. Ismail, B. Christina and L. J. Mauer, *J. Food Sci.*, 2018, **83**, 670–681.
64 S. Ghanbarzadeh, R. Hariri, M. Kouhsoltani, J. Shokri, Y. Javadzadeh and H. Hamishehkar, *Colloids Surfaces B Biointerfaces*, 2015, **136**, 1004–1010.
65 P. Bandyopadhyay and F. Rodriguez, *Polymer (Guildf).*, 1972, **13**, 119–123.
66 K. D. Gilroy, A. Ruditskiy, H.-C. Peng, D. Qin and Y. Xia, *Chem. Rev.*, 2016, **116**, 10414–10472.
67 M. Wuithschick, A. Birnbaum, S. Witte, M. Sztucki, U. Vainio, N. Pinna, K. Rademann, F. Emmerling, R. Kraehnert and J. Polte, *ACS Nano*, 2015, **9**, 7052–7071.

View Article Online
DOI: 10.1039/D0CE00826E

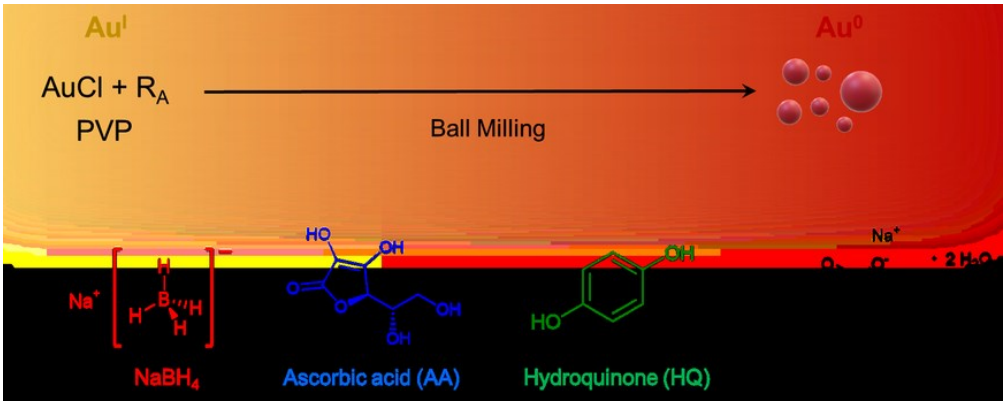

73x29mm (300 x 300 DPI)